CDK promotes interactions of Sld3 and Drc1 with Cut5 for initiation of DNA replication in fission yeast

Masayoshi Fukuura[a], Koji Nagao[b], Chikashi Obuse[b], Tatsuro S. Takahashi[a], Takuro Nakagawa[a], and Hisao Masukata[a]

[a]Graduate School of Science, Osaka University, Osaka 560-0043, Japan; [b]Graduate School of Life Science, Hokkaido University, Sapporo 001-0021, Japan

ABSTRACT **Cyclin-dependent kinase (CDK) plays essential roles in the initiation of DNA replication in eukaryotes. Although interactions of CDK-phosphorylated Sld2/Drc1 and Sld3 with Dpb11 have been shown to be essential in budding yeast, it is not known whether the mechanism is conserved. In this study, we investigated how CDK promotes the assembly of replication proteins onto replication origins in fission yeast. Phosphorylation of Sld3 was found to be dependent on CDK in S phase. Alanine substitutions at CDK sites decreased the interaction with Cut5/Dpb11 at the N-terminal BRCT motifs and decreased the loading of Cut5 onto replication origins. This defect was suppressed by overexpression of *drc1*$^{+}$. Phosphorylation of a conserved CDK site, Thr-111, in Drc1 was critical for interaction with Cut5 at the C-terminal BRCT motifs and was required for loading of Cut5. In a yeast three-hybrid assay, Sld3, Cut5, and Drc1 were found to form a ternary complex dependent on the CDK sites of Sld3 and Drc1, and Drc1–Cut5 binding enhanced the Sld3–Cut5 interaction. These results show that the mechanism of CDK-dependent loading of Cut5 is conserved in fission yeast in a manner similar to that elucidated in budding yeast.**

Monitoring Editor
Daniel Lew
Duke University

Received: Dec 21, 2010
Revised: Apr 28, 2011
Accepted: May 9, 2011

INTRODUCTION

In eukaryotes, the initiation of chromosome replication is tightly regulated during the cell cycle to ensure faithful duplication of the entire genome (Bell and Dutta, 2002; Diffley, 2004; Machida *et al.*, 2005). Cyclin-dependent kinase (CDK), whose activity is low in G1 phase and increases at the beginning of S phase, plays a major role in this regulation. In G1 phase, mediated by the ORC complex as well as Cdc6 and Cdt1, the Mcm2-7 complex, which is considered to be a core component of replicative helicase, is loaded onto replication origins to form prereplicative complexes (preRCs) (Diffley *et al.*, 1994; Bell and Dutta, 2002; Remus *et al.*, 2009). At the onset of S phase, CDK together with Dbf4-dependent kinase (DDK), which is another essential kinase for DNA replication, promotes the recruitment of several factors, including GINS and Cdc45, to preRCs for activation of Mcm2-7 helicase (Tanaka *et al.*, 2007; Zegerman and Diffley, 2007; Sheu and Stillman, 2010). Thereafter, Cdc45, GINS, and Mcm2-7 form a stable complex, called the CMG complex (Moyer *et al.*, 2006), which travels with DNA polymerases along chromosome DNA (Gambus *et al.*, 2006; Pacek *et al.*, 2006).

Recent studies of budding yeast have demonstrated that two replication proteins, Sld2/Drc1 and Sld3, are the key substrates of CDK for initiation of replication. Dpb11, which has two sets of tandem BRCT motifs that bind to phosphopeptides (Glover *et al.*, 2004), binds to phosphorylated Sld2 and Sld3 at C- and N-terminal BRCT motifs, respectively (Masumoto *et al.*, 2002; Tanaka *et al.*, 2007; Zegerman and Diffley, 2007). These interactions are the minimum requirements for CDK-dependent initiation of DNA replication in budding yeast. Sld3 binds to replication origins in G1 phase (Kamimura *et al.*, 2001; Kanemaki and Labib, 2006), whereas Dpb11 is loaded in S phase (Masumoto *et al.*, 2000). Thus phosphorylation of Sld3 may promote loading of Dpb11 via its direct interaction. On the other hand, the significance of Sld2 phosphorylation for assembly of replication proteins onto origins has yet to be elucidated. In addition to CDK, recent studies of budding yeast have shown that

This article was published online ahead of print in MBoC in Press (http://www.molbiolcell.org/cgi/doi/10.1091/mbc.E10-12-0995) on May 18, 2011.

Address correspondence to: Hisao Masukata (masukata@bio.sci.osaka-u.ac.jp).

Abbreviations used: CDK, cyclin-dependent kinase; DDK, Dbf4-dependent kinase; preRC, prereplicative complex.

the checkpoint kinase regulates the functions of Sld3 (Lopez-Mosqueda *et al.*, 2010; Zegerman and Diffley, 2010). Checkpoint activation upon DNA damage or replication fork stalling inhibits the initiation of replication at late origins. Rad53 kinase, which is a homologue of metazoan Chk2 and fission yeast Cds1, phosphorylates Sld3, and this inhibits the CDK-dependent interaction of Sld3 with Dpb11. Therefore Sld3 seems to be a crucial factor in the regulation of origin firing.

Although Sld2, Sld3, and Dpb11 play key roles in CDK-dependent regulation of replication, it is not known how the mechanism is conserved. In multicellular organisms, a plausible orthologue of Sld2 has been identified. RecQL4, a member of the metazoan RecQ helicase family, has a similarity to Sld2 in its amino terminus and is required for initiation of DNA replication in *Xenopus* egg extracts (Sangrithi *et al.*, 2005; Matsuno *et al.*, 2006). Although RecQL4 interacts with Cut5/TopBP1, an orthologue of Dpb11, this interaction does not depend on phosphorylation by CDK (Matsuno *et al.*, 2006). Unlike Sld2, RecQL4 appears to function after Cdc45 loading. Recently, three possible counterparts of Sld3 have been identified in multicellular organisms. Treslin/Ticcr, GEMC1, and DUE-B interact with TopBP1 and are required for loading of Cdc45 onto chromatin in *Xenopus* egg extracts (Balestrini *et al.*, 2010; Chowdhury *et al.*, 2010; Kumagai *et al.*, 2010; Sansam *et al.*, 2010). Although they share similarities with Sld3, the significance of their interactions with TopBP1 remains unknown.

Both Sld2 and Sld3 appear to have diversified during evolution, because their sequences are poorly conserved, even within fungi. Species of fission yeast, which are evolutionally distant from budding yeast, have both Sld3 and Drc1/Sld2, although they are barely identifiable by searches for sequence similarity. In fission yeast, Sld3 is essential for initiation of replication and is phosphorylated in a cell cycle–dependent manner (Nakajima and Masukata, 2002). Loading of Sld3 onto replication origins is dependent on DDK but not on CDK, which is required for subsequent recruitment of Cut5/Dpb11, GINS, Drc1, and Cdc45 (Yabuuchi *et al.*, 2006). Thus Sld3 may play critical roles at the intersection between DDK and CDK regulation. Fission yeast Drc1, which is essential for DNA replication, is phosphorylated by CDK, and the phosphorylation is required for interaction with Cut5 (Noguchi *et al.*, 2002). However, it has not been clarified whether Sld3 plays a role in regulation by CDK and how phosphorylation of Drc1 contributes to the assembly of replication proteins at origins.

In this study, we investigated the interaction of fission yeast Sld3 with Mcm2 and Cut5 in a yeast two-hybrid assay. The C-terminal region of Sld3 was shown to interact with the N-terminal BRCT motifs of Cut5, depending on the CDK sites of Sld3. Sld3 was phosphorylated in S phase in a CDK-dependent manner, and the phosphorylation was important for loading of Cut5 onto origins. We also showed that a CDK consensus site in a conserved region of Drc1 was phosphorylated within cells and required for interaction with the C-terminal BRCT motifs of Cut5 and for loading of Cut5 onto replication origins. Furthermore, Sld3, Cut5, and Drc1 were shown to form a ternary complex in yeast three-hybrid assays. These results suggest that CDK regulates the formation of Sld3–Cut5–Drc1 complexes at replication origins and the mechanism of CDK regulation is conserved between fission yeast and budding yeast.

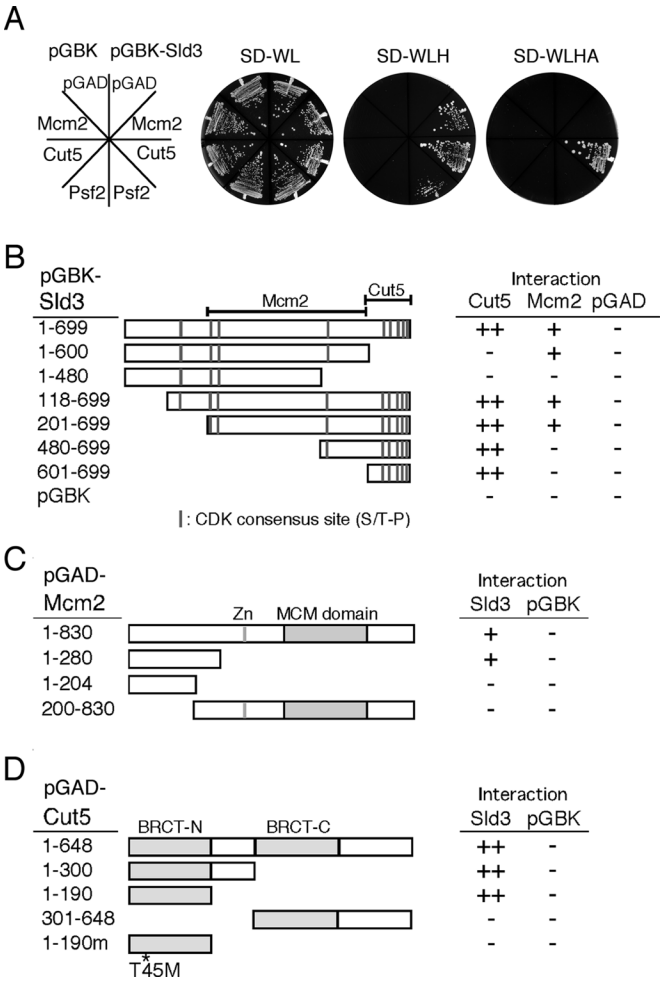

FIGURE 1: Sld3 binds to the amino-terminal region of Mcm2 and BRCT-N of Cut5 in a two-hybrid assay. (A) The results of two-hybrid analysis for interactions of Sld3 with Mcm2, Cut5, and Psf2 are presented. Yeast cells harboring either pGBKT7 or pGBKT7-Sld3 in combination with pGADT7-Mcm2, pGADT7-Cut5, or pGADT7-Psf2 were streaked on nonselective SD-WL and selective SD-WLH and SD-WLHA plates and incubated for 4 d at 30°C. (B) The results of two-hybrid assays for pGBKT7 carrying the full-length or truncated Sld3 and pGADT7 carrying Cut5 or Mcm2 are summarized. Positions of Sld3 fragments tested are schematically presented, together with locations of the CDK consensus sites (S/T-P) (vertical lines). Interactions as detected by growth on SD-WLH and SD-WLHA plates are shown by + and ++ signs, respectively. (C) Interactions between the full-length Sld3 cloned on pGBKT7 and full-length or partial fragments of Mcm2 on pGADT7 were analyzed using two-hybrid assays. Positions of Mcm2 fragments tested are schematically shown, together with locations of a zinc-finger motif (Zn) and the MCM domain. A plus sign (+) indicates growth on SD-WLH plates. (D) Interactions between fragments of Cut5 cloned on pGADT7 and the full-length Sld3 on pGBKT7 were analyzed using two-hybrid assays. The fragments of Cut5 and locations of BRCT-N and BRCT-C motifs are schematically shown. The position of the T45M substitution in the temperature-sensitive *cut5-T401* allele is shown by an asterisk. Growth on SD-WLHA plates is indicated by ++.

RESULTS

Sld3 binds to Mcm2 and Cut5 in a two-hybrid assay

To elucidate the roles of Sld3 in the initiation of DNA replication, we investigated interactions with Mcm2-7 subunits, GINS components (Psf1, Psf2, Psf3, Sld5), Cut5, Drc1, Mcm10, and Cdc45 using a yeast two-hybrid assay. Sld3 showed strong interactions with Mcm2 and Cut5 and a weak interaction with Psf2 (Figure 1A and Supplementary Table S1). To identify the regions of Sld3 required for the interactions with Mcm2 and Cut5, various segments were examined in two-hybrid assays (Figure 1B). The C-terminal region

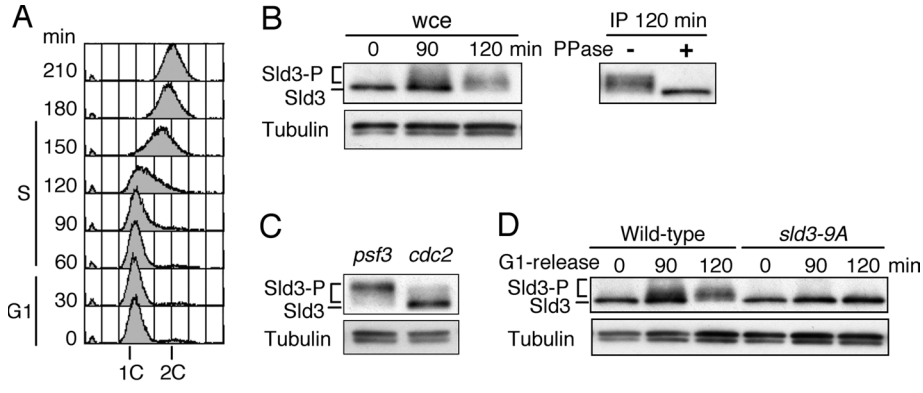

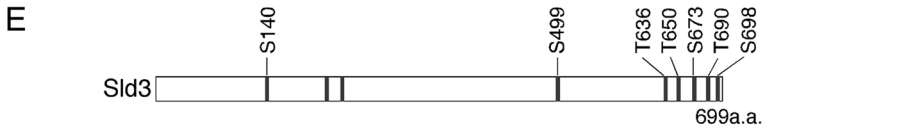

Phosphorylation Site	Sequence	Charge	Measured (m/z)	Caluculated (m/z)
S140	135-SNSLMS(Phos)PSLLK-145	+2	629.0	628.8
S499	484-ALPGNTSGASISNTSS(Phos)PHSEASISKDYEILK-514	+3	1081.9	1081.2
T636	624-SEPSMDSILVQAT(Phos)PR-638	+2	856.7	855.9
T650	640-SSSVITELPDT(Phos)PIK-653	+2	783.9	783.9
S673	660-ASACTVENHIVTES(Phos)PAHK-677	+2	1016.5	1016.0
T690	681-AQLFVCVPTT(Phos)PVK-693	+2	770.4	770.4
S698	696-SAS(Phos)PHM(Oxi)DYK-704	+2	566.4	566.2

Phos: Phosphorylation, Oxi: Oxidation

FIGURE 2: Phosphorylation of Sld3 during S phase, dependent on CDK. (A) The *sld3-flag cdc10-129* cells were arrested in G1 phase and released synchronously at 20°C to examine cell cycle–dependent phosphorylation of Sld3. The results of flow cytometry analysis are shown, along with positions of 1C and 2C DNA. (B) Proteins in cell extracts (wce) were prepared at 0, 90, and 120 min. Sld3-FLAG and α-tubulin were analyzed by immunoblotting with anti-FLAG and anti–α-tubulin antibodies (top). Positions of hyperphosphorylated and hypophosphorylated forms of Sld3 are shown. Immunoprecipitated Sld3-FLAG from the 120-min sample was incubated with or without λ protein phosphatase (PPase, right). (C) *nda3-KM311 psf3-1* (*psf3*) and *nda3-KM311 cdc2-33* (*cdc2*) cells arrested in M phase were released synchronously at 36°C. Sld3-FLAG and α-tubulin in cell extracts at 120 min after the release were analyzed by immunoblotting with anti-FLAG and anti–α-tubulin antibodies. (D) The *sld3-flag cdc10-129* (wild-type) and *sld3-9A-flag cdc10-129* (*sld3–9A*) cells were arrested in G1 phase and released synchronously at 20°C to examine cell cycle–dependent phosphorylation of Sld3. Proteins in cell extracts prepared at 0, 90, and 120 min were analyzed by immunoblotting with anti-FLAG and anti–α-tubulin antibodies. Positions of hyperphosphorylated and hypophosphorylated Sld3 are shown. (E) Positions of CDK sites that were identified as phosphorylated form by mass spectrometry analysis of Sld3 are indicated above the schematic presentation of phosphoreceptor serines/threonines in the CDK consensus sites (vertical lines). The phosphorylated polypeptides are listed along with their first and last positions, the state of charge, the measured m/z, and calculated m/z (bottom). The underlined amino acids in the polypeptide containing S698 are derived from a FLAG-tag cassette. The phosphorylation sites were validated by manual assignment of the observed MS/MS ions (Supplementary Figure S2B).

(601–699 amino acids) of Sld3 was sufficient for the interaction with Cut5, whereas the central region was required for the interaction with Mcm2 (Figure 1B). Deletion analysis of Mcm2 revealed that the N-terminal region (1–280 amino acids) was required for the interaction with Sld3 (Figure 1C).

The C-terminal region of Sld3 that interacts with Cut5 contains multiple CDK consensus sites. Therefore we investigated whether BRCT motifs of Cut5 interacted with Sld3. N-terminal fragments of Cut5 containing BRCT-N interacted with Sld3, whereas C-terminal fragments containing BRCT-C did not (Figure 1D). Accordingly, these results demonstrated that BRCT-N is required for the interaction with Sld3. Because the Thr45Met substitution responsible for the temperature sensitivity of *cut5-T401*, which has a defect in DNA replication (Saka *et al.*, 1997), abolished the interaction of BRCT-N with Sld3 (Figure 1D), the interaction may play an important role in the initiation of DNA replication.

Phosphorylation of Sld3 is dependent on CDK during S phase

Because Sld3 contains multiple CDK consensus sites (Figure 1A), we examined whether Sld3 is phosphorylated during S phase. Cells carrying *flag*-tagged *sld3* were arrested in G1 phase by the temperature-sensitive *cdc10-129* mutation and synchronously released. The results of flow cytometry showed that DNA replication occurred during 90–180 min after release (Figure 2A). Immunoblotting with anti-FLAG antibody showed that Sld3 in G1-phase cell extracts (0 min) migrated as a sharp band (Figure 2B). In contrast, at 90–120 min, corresponding to S phase, Sld3 migrated as multiple slower-moving bands (Figure 2B). Treatment with λ protein phosphatase resulted in a sharp, rapidly migrating band (Figure 2B, right, PPase +). These results show that Sld3 is phosphorylated in S phase.

To examine whether phosphorylation of Sld3 depends on CDK activity, *cdc2-33* high-temperature sensitive cells, in which CDK kinase activity is decreased (Booher *et al.*, 1989), were synchronized at M phase by a *nda3-KM311* cold-sensitive mutation and released at the restrictive temperature of *cdc2-33* to cause arrest at the G1/S boundary (Supplementary Figure S1). Cells carrying the temperature-sensitive mutation *psf3-1* in a GINS subunit were similarly arrested with 1C DNA content (Supplementary Figure S1; Yabuuchi *et al.*, 2006). On immunoblotting, Sld3 in *psf3-1* migrated as hyperphosphorylated forms (Figure 2C, *psf3*), whereas the majority of Sld3 migrated as hypophosphorylated forms in *cdc2-33* (Figure 2C, *cdc2*). These results show that Sld3 is phosphorylated in a CDK-dependent manner. To examine whether the predicted CDK consensus sites are required for phosphorylation of Sld3, serines or threonines of CDK-phosphoreceptor sites (S/T-P) of Sld3 were substituted by alanine residues at all nine sites (*sld3-9A*). The Sld3-9A protein appeared as a sharp, rapidly migrating band at 90–120 min after release, suggesting that the substitutions eliminated phosphorylation (Figure 2D). Taken together, the data indicate that CDK phosphorylates Sld3 during S phase.

To obtain direct evidence that CDK sites of Sld3 are phosphorylated in fission yeast cells, we carried out tandem mass spectrometry analysis of Sld3-FLAG that was immunoprecipitated from asynchronously cultured cells (Supplementary Figure S2A). The results of the spectrum analysis of tryptic peptides showed that S140, T636, T650, S673, and T690 were indeed phosphorylated (Figure 2E and supplementary Figure S2B). In addition, manual validation of phosphopeptides containing S449 or S698 supported that these residues

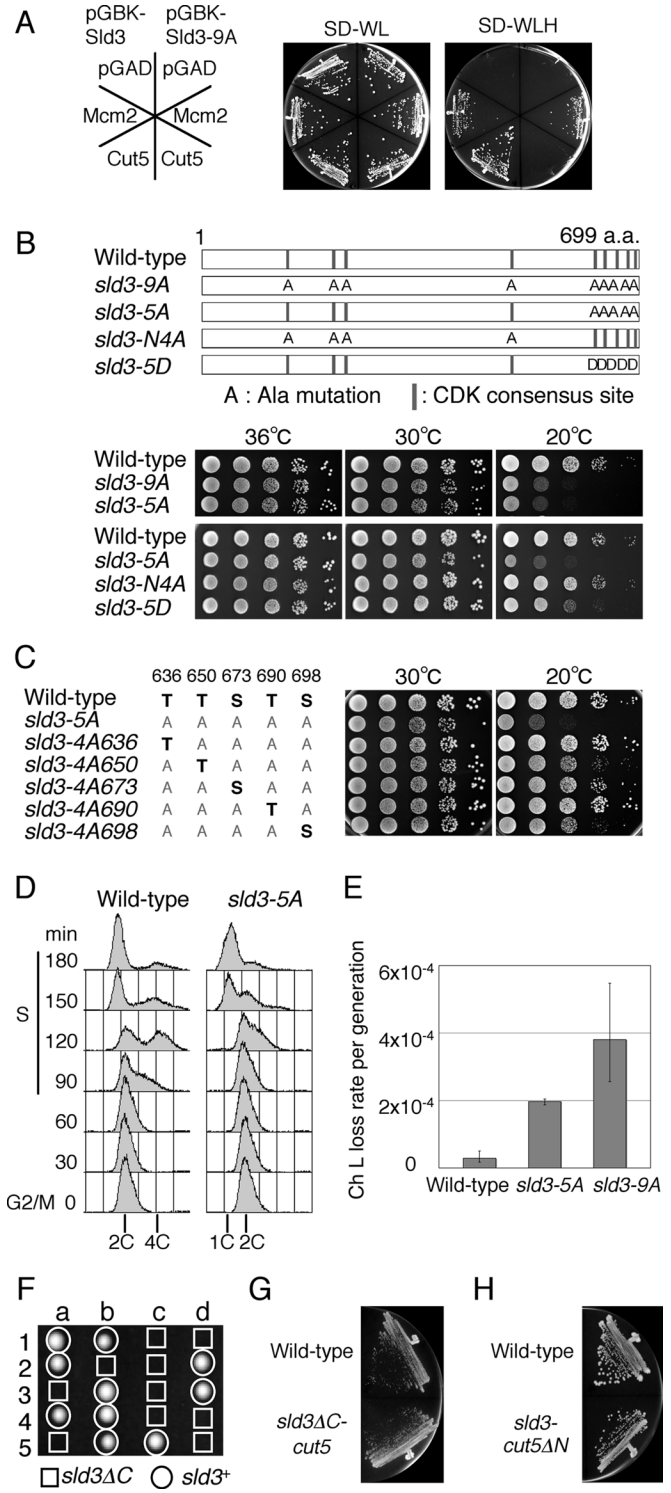

FIGURE 3: CDK consensus sites in Sld3 are required for efficient DNA replication. (A) The results of two-hybrid analysis between pGBKT7 carrying the wild-type *sld3* and *sld3-9A* with alanine substitutions at nine CDK sites and pGADT7 containing Mcm2 or Cut5. Yeast cells were incubated for 4 d at 30°C. (B) Locations of CDK consensus sites (S/T-P, vertical lines) and amino acid substitutions in *sld3* mutants are schematically shown. Alanine and aspartic acid substitutions are indicated by A and D, respectively. Fission yeast strains carrying *sld3*$^+$ (wild type) or *sld3* with alanine or aspartic acid substitutions were serially diluted and incubated on YE3S plates at the indicated temperature (bottom). (C) Cold sensitivity of strains carrying four-alanine substitutions were analyzed as described in B. The amino acids at the five CDK sites are indicated as S/T and A for wild type and alanine, respectively. (D) Wild-type and *sld3-5A* cells arrested at the G2/M boundary by the *cdc25-22* mutation were released at 20°C, and DNA contents were analyzed by flow cytometry. Positions of 1C, 2C, and 4C DNA contents are shown. (E) Loss rates of the minichromosome Ch-L in wild-type, *sld3-5A*, and *sld3-9A* strains at 30°C were analyzed. Mean values obtained from 15 independent colonies are indicated by vertical columns, with error bars showing 95% confidence ranges. (F) Results of tetrad analysis of *sld3*$^+$/*sld3ΔC-kan* diploid cells are presented. Spores (a–d) from five asci (1–5) were separated on YE3S plates and grown at 30°C. Squares and circles indicate the presence and absence of *sld3ΔC-kan*, respectively, as judged by sensitivity to kanamycin. (G) MF62 *sld3ΔC-cut5 cut5::kanMX6*, in which *sld3* lacking its C-terminal 601–699 region, was fused with the full length of *cut5*$^+$, and the wild-type strain were streaked on YE3S plates and incubated at 30°C. (H) MF48 *sld3-cut5ΔN cut5::kanMX6*, in which full length *sld3*$^+$ was fused with *cut5* lacking the N-terminal BRCT repeats (1–190 amino acids), and wild-type strain were streaked on YE3S plates and incubated at 30°C.

were likely to be phosphorylated (Figure 2E and supplementary Figure S2B). We could not determine whether T201 and T228 were phosphorylated because the tryptic peptides containing these sites were too long for the analysis. These results suggest that at least seven among nine predicted CDK sites of Sld3 are phosphorylated in fission yeast cells.

Importance of CDK phosphorylation of Sld3 for DNA replication and genome stability

Because Sld3 interacts with the BRCT motifs of Cut5, we investigated the role of Sld3 phosphorylation in the interaction with Cut5 using two-hybrid assays. Alanine substitutions in Sld3—9A impaired the interaction with Cut5 but did not affect the interaction with Mcm2 (Figure 3A), showing that the phosphorylation of Sld3 by CDK is required for interaction with Cut5.

If the interaction of Sld3 with Cut5 is important for DNA replication, *sld3-9A* would be expected to have some defect in DNA replication. Consistent with this idea, *sld3-9A* showed cold-sensitive growth (Figure 3B). Because Sld3 interacts with Cut5 via its C-terminal region, we constructed *sld3* mutants carrying alanine substitutions at five sites in the C-terminal region (Figure 3B). *sld3-5A* showed cold-sensitive growth similar to that of *sld3-9A*, suggesting that CDK sites in the C-terminal region are important for the growth (Figure 3B). On the other hand, alanine substitutions at four CDK sites in the 1–600 region (*sld3-N4A*) did not cause significant defects in cell growth (Figure 3B). To examine whether phosphorylation at the CDK sites in the C-terminal region was important for the growth, we introduced phosphomimetic aspartic acid substitutions at five CDK sites in the C-terminal region. *sld3-5D* partially restored growth at the low temperature (Figure 3B).

To determine which CDK site(s) in the C-terminal region of Sld3 is required for growth at low temperature, four among five CDK sites were substituted into alanine residues and their growth was compared with those of wild type and *sld3-5A*. The *sld3-4A636*, *sld3-4A673*, or *sld3-4A690* carrying four substitutions except at T636, S673, or T690, respectively, did not show significant cold sensitivity (Figure 3C), suggesting that phosphorylation at any of T636, S673, or T690 is sufficient for the growth. In addition, *sld-4A650* or *sld3-4A698*, in which four sites except for T650 or S698, respectively, were substituted with alanine, showed less cold sensitivity than *sld3-5A* (Figure 3C), suggesting that S698 and T650 also contributed to the cell growth. These results indicate that phosphorylation at any of five CDK sites in the C-terminal region

of Sld3 contributes to cell growth, although some of them are more important than others.

To examine whether the growth defect of *sld3-5A* at low temperature was due to a defect in DNA replication, the DNA contents of *sld3-5A* cells were analyzed by flow cytometry. Wild-type and *sld3-5A* cells were arrested at the G2/M boundary by the *cdc25-22* mutation and released synchronously at 20°C. Wild-type cells showed an increase in their DNA content during 90–150 min after release (Figure 3D). In contrast, the DNA content of *sld3-5A* cells increased only slightly and cells with 1C DNA accumulated (Figure 3D), suggesting a defect in the early stage of DNA replication. These results suggest that CDK phosphorylation of Sld3 is required for efficient DNA replication.

Efficient initiation of DNA replication is required for maintenance of chromosomes (Patel *et al.*, 2008). To examine the effects of Sld3 phosphorylation on genome stability, we measured the stability of a minichromosome in the wild type, *sld3-5A*, and *sld3-9A* at a permissive temperature. The minichromosome Ch-L consists of part of chromosome III including the centromere and is stably maintained in wild-type cells (Nakamura *et al.*, 2008). The rates of loss of Ch-L in *sld3-5A* and *sld3-9A* at a permissive temperature of 30°C were 6.9- and 13-fold higher, respectively, than that in the wild type (Figure 3E). These results show that phosphorylation of Sld3 contributes to genome stability under conditions exerting no apparent growth defect.

Essential role of the C-terminal region of Sld3 is interaction with Cut5

Because phosphorylation of Sld3 is required for efficient DNA replication, we examined whether the interaction between Sld3 and Cut5 plays essential roles in the initiation of replication. The region of *sld3*$^+$ encoding the C-terminal 99 amino acids was deleted in a diploid strain (*sld3ΔC/sld3*$^+$), and growth of the progeny after meiosis was analyzed. Spores carrying *sld3ΔC* did not form colonies (Figure 3F), although microscopic analysis showed that they germinated and generated elongated cells after one or two rounds of cell division (unpublished data). These results show that the C-terminal region of Sld3 that interacts with Cut5 is essential for viability. If the essential role of the C-terminal region of Sld3 were solely to interact with Cut5, the requirement might be bypassed by tethering of Sld3ΔC with Cut5. Cells carrying an *sld3ΔC-cut5* fusion gene lacking both the endogenous *sld3*$^+$ and *cut5*$^+$ grew, albeit slightly more slowly than wild-type cells (Figure 3G). These results indicate that the essential role of the Sld3 C-terminal region is to interact with Cut5.

The BRCT-N of Cut5 is essential for cell growth (Saka *et al.*, 1994). If the essential role of this region is to interact with Sld3, then tethering of Sld3 to Cut5 might bypass this requirement. Indeed, *sld3-cut5ΔN* lacking the endogenous *sld3*$^+$ and *cut5*$^+$ grew (Figure 3H), indicating that the essential role of the BRCT-N is to interact with Sld3. Taking these together with the results for *sld3ΔC-cut5*, we conclude that the interaction between Sld3 and Cut5 is essential for viability.

CDK phosphorylation of Sld3 is important for loading of Cut5 onto replication origins

At the onset of S phase, Sld3 is required for loading of Cut5 onto origins, whereas the reverse is not the case (Yabuuchi *et al.*, 2006). Because loading of Cut5 depends on CDK activity, we hypothesized that phosphorylation-dependent interaction of Sld3 with Cut5 might promote loading of Cut5 onto origins. To test this idea, we examined the localization of Cut5 at replication origins at low temperature in *sld3-9A* using chromatin immunoprecipitation (ChIP) assays. The wild-type and *sld3-9A* derivatives carrying *sld3-flag* and *cut5-myc* were synchronously released from G2/M block to 20°C, the restrictive temperature for *sld3-9A*. DNA immunoprecipitated with Mcm6, Sld3-FLAG, and Cut5-myc was analyzed by qPCR for the *ars2004* locus, an efficient replication origin, and non-ARS, 30 kb away from the origin. In the wild type, Mcm6-IP recovery of *ars2004* was similar to that of non-ARS at the G2/M boundary (0 min), but it increased greatly at 80 min, followed by slight reduction at 100 min (Figure 4A, left), indicating preferential localization of Mcm6 at the origin during G1/S phase. In the *sld3-9A* mutant, recovery of *ars2004* by Mcm6-IP was increased at 80 min (Figure 4A, right). The signal increased further at later time points, probably due to accumulation of preRC without the initiation of replication. In the wild type, Sld3 showed significantly greater localization at *ars2004* than at the non-ARS locus at 80 and 100 min (Figure 4B, left). In *sld3-9A*, the mutant Sld3 protein was localized more efficiently at *ars2004* than was the case in the wild type (Figure 4B, right), indicating that phosphorylation of Sld3 was not required for loading of Sld3 onto the origin. This is consistent with the previous observation that Sld3 loading is dependent on DDK but not on CDK activity (Yabuuchi *et al.*, 2006).

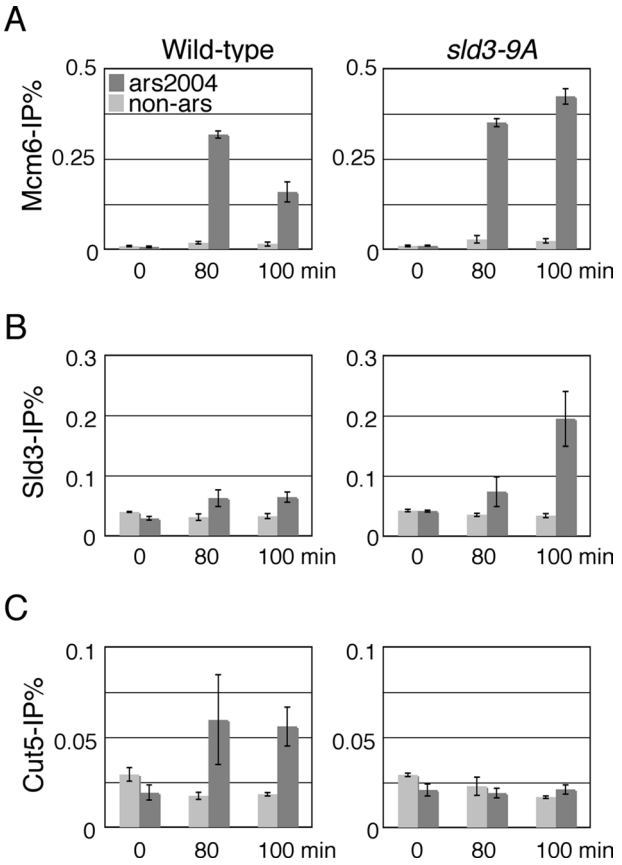

FIGURE 4: CDK consensus sites in Sld3 are required for the loading of Cut5 onto replication origins. (A–C) *sld3-flag cut5-myc* (wild type) and *sld3-9A-flag cut5-myc* (*sld3-9A*) cells were arrested at the G2/M boundary by the *cdc25-22* mutation and synchronously released at 20°C. DNA recovered by immunoprecipitation of Mcm6 (A), Sld3-FLAG (B), or Cut5-myc (C) at indicated time points was quantitated by real-time PCR using primers for *ars2004* and non-ARS loci. IP recovery (%) was calculated as IP DNA/total DNA. The average value of IP recovery obtained from two independent culture sets is shown by a vertical column with an error bar of standard deviations.

In the wild type, Cut5 was localized at *ars2004* two or three times more efficiently than at the non-ARS locus at 80–100 min, showing that Cut5 was loaded at the origin (Figure 4C, left). In contrast, Cut5 in *sld3-9A* cells was not localized at *ars2004* or non-ARS at any time point (Figure 4C, right). These results show that CDK phosphorylation of Sld3 is important for loading of Cut5 onto the origin.

Phosphorylation at a conserved CDK consensus site in Drc1 is required for interaction with Cut5

Drc1, a fission yeast homologue of Sld2, has been shown to be phosphorylated by CDK, and this phosphorylation is known to be required for interaction with Cut5 (Noguchi *et al.*, 2002). Although phosphorylation of Sld3 by CDK plays a role in loading of Cut5 onto replication origins, the functions of Drc1 phosphorylation are unknown. Of interest, we found that the cold sensitivity of *sld3-9A* was suppressed by overexpression of *drc1*$^+$ but not by *cut5*$^+$ (Figure 5A). These results imply that Drc1 plays a role in loading of Cut5 onto replication origin.

Fission yeast Drc1, a 337–amino acid protein that shares <20% sequence identity with budding yeast Sld2 (*Sc*Sld2), has 11 CDK consensus sites (Figure 5B). It has been shown that, in *Sc*Sld2, phosphorylation of threonine 84 (T84) in a noncanonical site among 11 possible CDK sites is essential for the interaction with Dpb11 and for viability (Tak *et al.*, 2006). Of interest, the amino acid sequence containing the threonine at position 111 (T111) in fission yeast Drc1 is conserved among fission yeast species and is homologous to those around the T84 of *Sc*Sld2 (Figure 5C). Therefore we investigated the role of Drc1 T111 in CDK-dependent regulation of initiation of DNA replication.

To determine whether T111 of Drc1 is phosphorylated in fission yeast cells, FLAG-Drc1 was immunoprecipitated from asynchronously cultured cells for analysis by mass spectrometry (Supplementary Figure S3A). The results of immunoblotting with anti-FLAG antibody showed that the treatment of immunoprecipitated FLAG-Drc1 with λ protein phosphatase resulted in rapidly migrating bands (Supplementary Figure S3B), indicating that the majority of Drc1 is phosphorylated. In tandem mass spectrometry analysis, the polypeptide containing phosphorylated T111 was detected (Figure 5D), indicating that T111 was indeed phosphorylated in fission yeast cells.

Next we examined requirement of T111 phosphorylation of Drc1 for the interaction with Cut5 using yeast two-hybrid assays. Drc1 showed interactions with the full-length Cut5, the N-terminal fragment (1–300) containing BRCT-N, and the C-terminal fragment (301–648) containing BRCT-C (Figure 5E and supplementary Figure S4). However, Drc1-T111A carrying an alanine substitution for T111 showed preferential decrease in the interaction with the C-terminal fragment, whereas a phosphomimetic glutamic acid substitution in Drc1-T111E restored the interaction (Figure 5E and supplementary Figure S4). These results suggest that the interaction of Drc1 with BRCT-C of Cut5 requires phosphorylation at T111.

Essential role of a conserved CDK consensus site of Drc1 in DNA replication and origin loading of Cut5

To examine whether phosphorylation at T111 of Drc1 plays an essential role in DNA replication, we constructed a strain carrying an extra copy of *drc1*$^+$ under the thiamine-repressible *Pnmt81* promoter at the *leu1* locus. The *drc1*Δ *Pnmt81-drc1*$^+$ strain in the presence of thiamine showed DNA replication block with accumulation of 1C DNA (Supplementary Figure S5) and defective growth on plates (Noguchi *et al.*, 2002). To examine the requirement of phosphorylation at T111, genomic *drc1*$^+$ was replaced with the

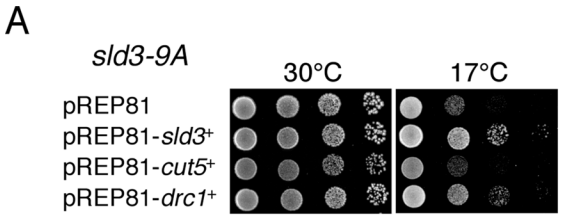

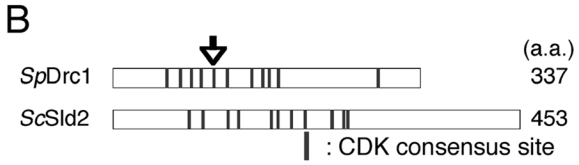

C

*Sc*Sld2	79	VEIGPTPQVYGK
*Sp*Drc1	106	SLLGPTPQLSRR
*Sj*Sld2	99	TILGPTPQLTRK
		:*****: :

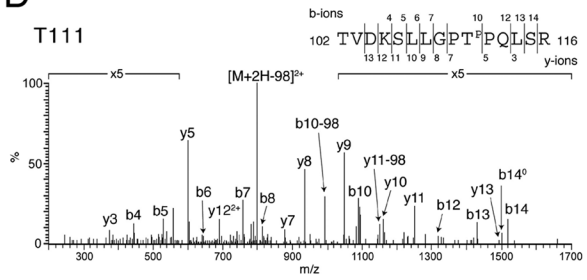

E

pGBK \ pGAD	Cut5-full	Cut5-1-300	Cut5-301-648	vector alone
Drc1	++	++	++	+
Drc1-T111A	++	++	+	+
Drc1-T111E	++	++	++	+

(+ : SD-WLH; ++ : SD-WLHA)

FIGURE 5: Phosphorylation at a conserved CDK consensus site of Drc1 is required for interaction with Cut5. (A) *sld3-9A leu1-32* cells harboring vector alone (pREP81), *sld3*$^+$ (pREP81-*sld3*$^+$), *cut5*$^+$ (pREP81-*cut5*$^+$), or *drc1*$^+$ (pREP81-*drc1*$^+$) were diluted serially, spotted on EMM plates, and incubated at the indicated temperature. (B) Locations of CDK consensus sites in *S. pombe* Drc1 (*Sp*Drc1) and in *S. cerevisiae* Sld2 (*Sc*Sld2) are schematically shown by vertical lines. An arrow indicates a conserved CDK site as described in C. (C) Amino acid sequences around a conserved CDK site in *Sc*Sld2, *Sp*Drc1, and *Schizosaccharomyces japonicus* (*Sj*Sld2) are presented. Asterisks and colons show identical and similar amino acids, respectively. A vertical arrow indicates phosphoreceptor threonine in the CDK consensus site. (D) Results of identification of Thr-111 phosphorylation by tandem mass spectrometry analysis are presented. MS/MS spectrum of the m/z 846.8 ion corresponding to phosphorylated peptide 102–116 of Drc1 is presented. The amino acid sequences and the spectra of respective b and y ions produced are shown. The phosphorylated threonine residue is indicated with P in the amino acid sequence. (E) Results of yeast two-hybrid assays for interactions between Drc1, Drc1-T111A, or Drc1-T111E on pGBKT7 and Cut5 fragments on pGADT7 are presented. Growth on SD-WLH and SD-WLHA is indicated by + and ++ signs, respectively.

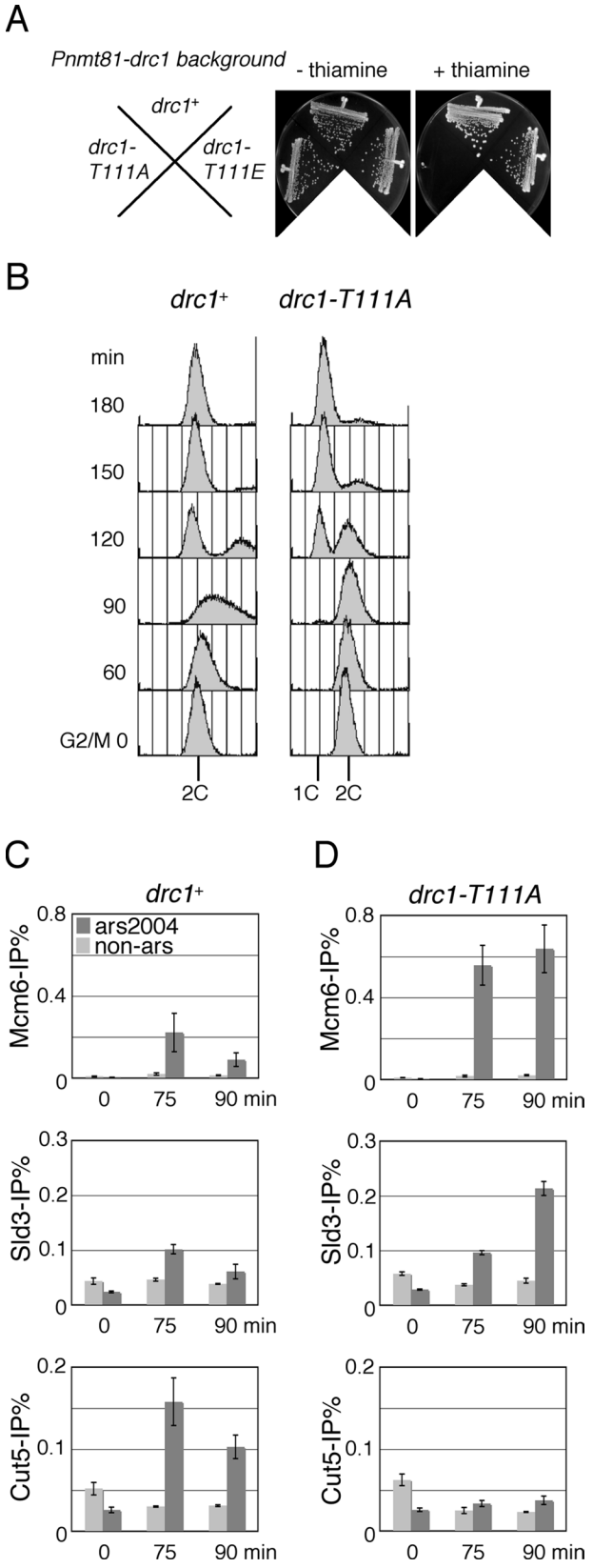

FIGURE 6: A conserved CDK site in Drc1 is required for loading of Cut5 onto replication origins. (A) *Pnmt81-drc1*$^+$ derivatives carrying *drc1*$^+$, *drc1-T111A*, and *drc1-T111E* alleles under native promoter control were streaked on EMM plates with (promoter off) or without (promoter on) thiamine (1 mg/ml). (B) For DNA content analysis, *cdc25-22* derivatives carrying *drc1*$^+$ or *drc1-T111A Pnmt81-drc1*$^+$ were cultured with thiamine (1 mg/ml) to repress the *Pnmt81* promoter for 5 h at 25°C. Cells arrested at the G2/M boundary were synchronously released at 25°C. (C, D) *cdc25-22 sld3-flag cut5-myc* derivatives carrying *drc1*$^+$ (C) or *drc1-T111A Pnmt81-drc1*$^+$ (D) were released from G2/M as described in B. At 0 (G2/M phase), 75 and 90 min (early S phase) after release, Mcm6 (top), Sld3-FLAG (middle), and Cut5-myc (bottom) were immunoprecipitated, and the amounts of *ars2004* and non-ARS regions recovered were measured by real-time PCR. The average value of IP recovery obtained from two independent culture sets is shown by a vertical column with an error bar of standard deviations.

drc1-T111A or *drc1-T111E* gene, carrying an alanine or glutamic acid substitution for T111, respectively, in the *drc1*Δ *Pnmt81-drc1*$^+$ strain. Under repression of *Pnmt81-drc1*$^+$, cells carrying *drc1-T111A* did not form colonies (Figure 6A). In contrast, cells with *drc1-T111E* carrying a phosphomimetic substitution did generate colonies, although they showed slightly slower growth than those carrying *drc1*$^+$ (Figure 6A). These results suggest that phosphorylation at T111 of Drc1 is essential for viability. We examined the DNA content of cells carrying *drc1*$^+$ or *drc1-T111A* released synchronously from G2/M block under repression of *Pnmt81-drc1*$^+$. In contrast to *drc1*$^+$ cells, where robust DNA replication occurred, as shown by a 2–4C DNA peak at 90–120 min, *drc1-T111A* cells formed a 1C DNA peak (Figure 6B), indicating that T111 of Drc1 is required for DNA replication.

Because overexpression of *drc1*$^+$ suppressed the growth defect of *sld3-9A*, we investigated whether T111 of Drc1 plays a role in the loading of Cut5 onto origins. Localization of Mcm6, Sld3-FLAG, and Cut5-myc was analyzed by ChIP in *drc1*$^+$ and *drc1-T111A* under repression of *Pnmt81-drc1*$^+$. In *drc1*$^+$ cells, Mcm6, Sld3, and Cut5 were localized at *ars2004* in early S phase and decreased later (Figure 6C). In *drc1-T111A*, by contrast, the localization of Cut5 was greatly decreased, whereas Mcm6 and Sld3 were efficiently localized at *ars2004* (Figure 6D). These results demonstrate that phosphorylation at T111 in Drc1 is required for loading of Cut5 onto replication origins.

Drc1 stimulates formation of the Sld3–Cut5–Drc1 complex

Because Sld3 and Drc1 interact with Cut5 at BRCT-N and BRCT-C, respectively, and both interactions are required for loading of Cut5 onto replication origins, a ternary complex of Sld3-Cut5-Drc1 could be formed dependently on CDK. To assess this possibility, we used yeast three-hybrid assays in which interactions between DB-Sld3 with AD-Drc1 were analyzed under expression of the third protein (Figure 7A). Interaction between DB-Sld3 and AD-Drc1 was not observed in the absence of Cut5 but was clearly observed in its presence (Figure 7B), indicating that Cut5 is required for the interaction between Sld3 and Drc1. The interaction was dependent on both the BRCT-N and BRCT-C motifs of Cut5 and was impaired by temperature-sensitive mutation (T45M) of *cut5* (Figure 7B). Furthermore, *sld3-9A* and *drc1-T111A* mutations, but not *drc1-T111E*, impaired the interaction (Figure 7C). These results suggest that Sld3, Cut5, and Drc1 form a ternary complex dependent on CDK phosphorylation of Sld3 and Drc1.

Because the cold sensitivity of *sld3-9A* was suppressed by overexpression of *drc1*$^+$ (Figure 5A), Drc1 is likely to contribute to interactions between Sld3 and Cut5. To assess this possibility, we used a yeast two-hybrid assay harboring DB-Sld3-9A and AD-Cut5 in the presence or absence of Drc1 expression. The growth of cells on plates testing for His expression was significantly increased by the presence of Drc1 (Figure 7D). These results are consistent with the idea that interaction of Drc1 with Cut5 stimulates association of

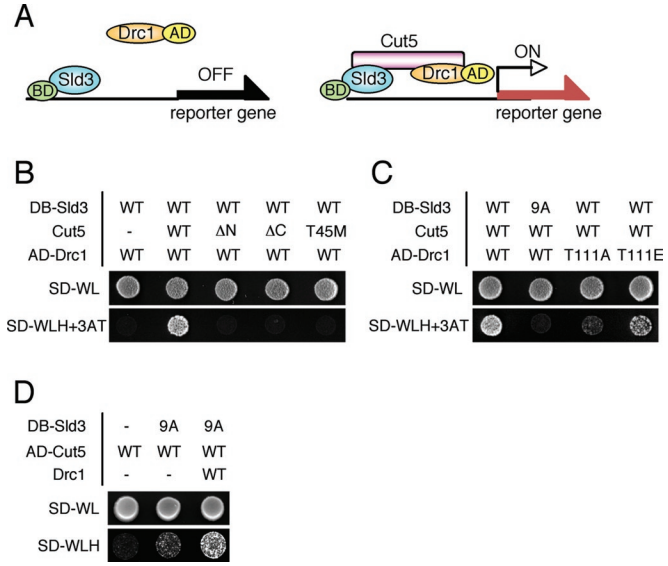

FIGURE 7: Drc1 stimulates the formation of Sld3–Cut5–Drc1 complexes. (A) Schematic illustration of the yeast three-hybrid assay. In the absence of physical interaction between DB-Sld3 and AD-Drc1, reporter genes are not expressed. In the presence of the third protein, Cut5, which simultaneously interacts with both DB-Sld3 and AD-Drc1, formation of a ternary complex allows expression of reporter genes. (B, C) For three-hybrid analysis, pBridge carrying DB-Sld3 or DB-Sld3–9A together with the third component Cut5 or its deletion derivative and pGADT7 carrying AD-Drc1, AD-Drc1-T111A, or AD-Drc1-T111E were introduced into AH109. Cultures of transformants were spotted on SD-WL and SD-WLH+3AT lacking histidine and containing 2 mM 3-aminotriazole. ΔN and ΔC lack 1–190 and 301–648 amino acids of Cut5, respectively. T45M indicates full-length Cut5 carrying the temperature-sensitive mutation. (D) In yeast two-hybrid analysis, a pBridge vector carrying DB-Sld3-9A with or without the third component, Drc1, was introduced together with pGADT7-Cut5 into AH109. Cultures of transformants were spotted on SD-WL and SD-WLH plates.

Cut5 with Sld3, resulting in loading of Cut5 onto replication origins dependent on CDK.

DISCUSSION

At the onset of S phase, CDK and DDK play crucial roles in initiation of DNA replication. In this study, we showed that CDK-dependent phosphorylation of Sld3 and Drc1 is required for their respective interactions with the N- and C-terminal BRCT motifs of Cut5. In addition, our results suggested stimulation of the Sld3–Cut5 interaction by Drc1–Cut5 interaction. Therefore both interactions are required for loading of Cut5 onto replication origins. These findings indicate that the role of CDK is to promote formation of the Sld3–Cut5–Drc1 complex at replication origins, whereas Sld3 is recruited to preRC dependent on DDK.

The mechanism of CDK-dependent loading of Cut5 onto origins

Sld3 is required for loading of Cut5, GINS, and Cdc45 onto replication origins (Yamada *et al.*, 2004; Yabuuchi *et al.*, 2006). Here, using yeast two-hybrid assays, we showed that the C-terminal region of Sld3 interacts with the N-terminal BRCT motifs of Cut5 (Figure 1, B and D). Both regions are essential for viability, and their roles are solely to interact with each other (Figure 3, F–H). The phosphorylation of Sld3 is important for loading of Cut5 onto replication origins (Figure 4C) and thus for efficient initiation of replication (Figure 3D). These findings suggest that CDK regulates the loading of Cut5 onto origins through phosphorylation-dependent interaction between Sld3 and Cut5.

Drc1 has been shown to be phosphorylated by CDK (Noguchi *et al.*, 2002). We found that phosphorylation of Thr-111 in a CDK site conserved among yeasts is essential for viability (Figure 6A). Although Drc1 interacts with the BRCT-N motifs (Noguchi *et al.*, 2002) and with the BRCT-C motifs of Cut5 in two-hybrid assays (Figure 5E), the interaction with BRCT-C was specifically impaired by T111A substitution and restored by T111E (Figure 5E). Noguchi *et al.* (2002) have shown that *drc1-CD5A*, which has alanine substitutions at five canonical CDK sites of Drc1, exhibits impaired interactions with BRCT-N. However, *sld3-cut5ΔN* cells are viable (Figure 3H), indicating that the interaction of Drc1 with BRCT-N is not essential. Thus the essential CDK-dependent interaction of Drc1 with Cut5 involves BRCT-C motifs.

It is not fully understood how phosphorylation of Drc1/Sld2 promotes assembly of replication proteins onto replication origins. In this study, we demonstrated that phosphorylation at T111 of Drc1 is required for loading of Cut5 onto replication origins (Figure 6D). Therefore CDK regulates the loading of Cut5 onto origins through not only phosphorylation of Sld3, but also phosphorylation of Drc1. Furthermore, we found that Sld3, Cut5, and Drc1 form a complex in three-hybrid assays (Figure 7B). Overexpression of Drc1 suppressed the growth defect of *sld3-9A* cells, and expression of Drc1 enhanced the interaction of Sld3-9A with Cut5 in two-hybrid assays (Figure 7D). Because the enhancement was dependent on T111 of Drc1 (unpublished data), the interaction of Drc1 with Cut5 at BRCT-C may stimulate the interaction of BRCT-N motifs with Sld3.

We have previously shown that GINS is required for origin loading of Drc1 and that overexpression of *drc1*$^+$ suppresses the growth defect of *psf3-1* (Yabuuchi *et al.*, 2006), suggesting that Drc1 may act together with GINS. Because loading of GINS is dependent on Cut5 and CDK, the results that loading of Cut5 is dependent on Drc1 shown in this study are consistent with the idea that all of GINS, Cut5, and Drc1 are mutually interdependent for origin loading and that all are CDK-dependent. This is further supported by the results of ChIP analysis showing that loading of Drc1 is dependent on CDK, using the temperature-sensitive *cdc2-33* mutant (Y. Yamada and H. Masukata, unpublished data). A recent study of budding yeast showed that a preloading complex containing Dpb11, Sld2, GINS, and Polε is formed in a CDK-dependent manner (Muramatsu *et al.*, 2010). It remains to be investigated how GINS and Polε contribute to origin loading.

CDK together with DDK is required for assembly of replication factors at origins during S phase. In *sld3-9A* or *drc1-T111A* mutants, CDK-dependent loading of Cut5 onto replication origin does not occur, whereas Sld3 is localized (Figures 4 and 6). These results are consistent with the previous observation that loading of Sld3 onto origins does not depend on CDK but rather on DDK (Yabuuchi *et al.*, 2006). Some DDK-dependent interaction between Sld3 and a preRC component should play a role in this process. In this regard, the interaction of Sld3 with the N-terminal region of Mcm2 observed in two-hybrid assays is of interest (Figure 1C). Also of interest, in *Saccharomyces cerevisiae* the N-terminal 1–278 amino acids of Mcm2 contain DDK phosphorylation sites as well as a docking site (Bruck and Kaplan, 2009). Therefore DDK-dependent phosphorylation on MCM subunits may enhance the interaction between Sld3 and Mcm2 for loading of Sld3 onto replication origins.

Conservation of mechanisms for CDK-dependent chromosomal DNA replication

Initiation of DNA replication is regulated by CDK in all eukaryotes. However, it is not known how the mechanism of regulation is conserved. We have showed that CDK regulates the initiation of replication via phosphorylation of Sld3 and Drc1/Sld2 in an organism other than budding yeast. Phosphorylation of Sld3 and Drc1 is required for interactions with respective BRCT motifs of Cut5 to promote formation of a ternary Sld3–Cut5–Drc1 complex. The framework of the regulation appears to be very much conserved (Tanaka *et al.*, 2007; Zegerman and Diffley, 2007). The many conserved features include interactions of the N- and C-terminal bipartite BRCT motifs of Cut5/Dpb11 with Sld3 and Drc1/Sld2, respectively, and the essential nature of a noncanonical CDK site in Drc1/Sld2.

The present study of fission yeast Sld3 showed that phosphorylation at any of T636, S673, or T690 was sufficient for the growth (Figure 3C). Of interest, a valine residue is present at the −3 position of these phosphoreceptor sites. Because this signature also exists at T600, one of two critical CDK sites of budding yeast Sld3, and at T215 phosphoreceptor site of fission yeast Crb2, which interacts with BRCT-N of Cut5 (Esashi and Yanagida, 1999; Du *et al.*, 2006), it may be required for efficient interaction with Cut5/Dpb11 at the N-terminal BRCT motifs.

An essential replication protein, Cut5/Dpb11/TopBP1, containing multiple BRCT domains is conserved from yeast to humans (Garcia *et al.*, 2005). TopBP1 is required for loading of GINS and Cdc45 chromatin (Hashimoto and Takisawa, 2003; Kubota *et al.*, 2003). Recently, novel TopBP1-interacting proteins that are required for DNA replication have been discovered. One such protein, Treslin, shares several common features with fungal Sld3 (Kumagai *et al.*, 2010). First, Treslin interacts with TopBP1 in the BRCT I-II region that is most similar to BRCT-N of Cut5. Second, association of Treslin with chromatin is dependent on preRC but not on TopBP1 or CDK activity. Third, Treslin is required for association of GINS and Cdc45 with chromatin. Finally, a segmental amino acid sequence of Treslin shows significant similarity with the middle region of fungal Sld3 (Sanchez-Pulido *et al.*, 2010). It is plausible that Treslin is a functional orthologue of Sld3 in multicellular organisms. Another candidate orthologue of Sld3 is GEMC1 (Balestrini *et al.*, 2010), which interacts with TopBP1 and Cdk2-cyclin E. Phosphorylation of GEMC1 stimulates its interaction with TopBP1 and initiation of replication. Therefore, although the functions of RecQL4 seem to differ from that of fungal Drc1/Sld2, metazoan Sld3 orthologues may play a crucial role in the well-conserved underlying mechanism of CDK-dependent DNA replication from yeast to humans.

MATERIALS AND METHODS

Strains and media

Fission yeast strains were cultured in complete YE medium (0.5% yeast extract, 3% glucose) and minimal EMM medium (Moreno *et al.*, 1991). Media containing 2% agar were used for plating. *Schizosaccharomyces pombe* strains and PCR primers used in this study are listed in Tables 1 and 2, respectively.

The *sld3* mutant genes carrying amino acid substitutions were constructed as follows. A 184–base pair fragment of the downstream noncoding region of *sld3*$^+$ was PCR amplified from the genomic DNA of wild-type HM19 using primers P1 and P2 and cloned into the *Eco*RI-*Kpn*I sites of pBluescript II KS+ to make pBS-DW. A *Bam*HI-*Pst*I fragment containing the polyadenylation signal of the *nmt1* gene and a *Bgl*II-*Eco*RI fragment containing *kanMX6* were inserted together with a linker DNA made by annealing of oligonucleotides P3 with P4, thus creating the *Sma*I site disrupting the *Pst*I and *Bgl*II sites, into the *Bam*HI-*Eco*RI sites of pBS-DW to make pBS-kanMX6-DW. A *Spe*I-*Bam*HI fragment encoding the 65th amino acid to the C-terminal end of Sld3 of pREP81-*sld3* (Nakajima and Masukata, 2002) was cloned into the *Spe*I-*Bam*HI sites of pBS-kanMX6-DW to form pBS-*sld3*-kan-DW. pBS-*sld3-4A636*-kan-DW was made by replacing the *Bam*HI fragment (encoding 344–699 amino acids) of pBS-*sld3*-kan-DW with a PCR-amplified fragment using primer P23 and P24 from pREP81-*sld3-T650A-S673A* (R. Nakajima and H. Masukata, unpublished data). pBS-*sld3-4A650*-kan-DW was similarly constructed using pREP81-*sld3-T636A-S673A* for PCR reaction. pBS-*sld3-4A673*-kan-DW or pBS-*sld3-4A690*-kan-DW was made by similar replacement with a PCR-amplified fragment using primer P23 or P25 from pREP81-*sld3-T636A-T650A-T690A* or pREP81-*sld3-T636A-T650A-S673A*, respectively. pBS-*sld3-4A698*-kan-DW was made by replacing the *Xho*I-*Bam*HI fragment of pBS-*sld3*-kan-DW with the corresponding fragment of pREP81-*sld3-4A* carrying substitutions T636A, T650A, S673A, and T690A (Nakajima and Masukata, 2002). pBS-*sld3-5A*-kan-DW was made by similar replacement with a *Xho*I-*Bam*HI fragment PCR amplified from pREP81-*sld3-4A* using primers P5 and P6 to add S698A substitution. To construct pBS-*sld3-9A*-kan-DW, the *Spe*I-*Bam*HI (internal site in *sld3*$^+$) carrying substitutions S140A, T201A, and T228A made by PCR amplifications using primer sets P5 and P7, P5 and P8, and P9 and P10 and the *Bam*HI (internal)-*Stu*I fragment carrying a substitution S499A amplified using primers P9 and P10 were inserted in place of the *Spe*I-*Stu*I fragment of pBS-*sld3*-kan-DW. The *Xho*I-*Kpn*I fragments of pBS-*sld3-4A*-kan-DW and pBS-*sld3-5A*-kan-DW or the *Spe*I-*Kpn*I fragments of pBS-*sld3-4A636*-kan-DW, pBS-*sld3-4A650*-kan-DW, pBS-*sld3-4A673*-kan-DW, pBS-*sld3-4A690*-kan-DW, and pBS-*sld3-9A*-kan-DW were used to transform HM19. Among G418-resistant transformants, integration of *sld3-4A636*, *sld3-4A650*, *sld3-4A673*, *sld3-4A690*, *sld3-4A698*, *sld3-5A*, or *sld3-9A* genes at the *sld3*$^+$ locus was confirmed by PCR and genomic sequencing, resulting in MF112, MF113, MF114, MF115, MF3, MF11, and MF7, respectively. pBS-*sld3-N4A-ura4*$^+$, pBS-*sld3-5A-ura4*$^+$, and pBS-*sld3-5D-ura4*$^+$ were constructed as just described except that *ura4*$^+$ was used instead of *kanMX6*, and used to generate MF26, MF31, and MF23. The *sld3-9A* was tagged at the C-terminus with a 5-FLAG epitope tag as described previously (Nakajima and Masukata, 2002). For construction of the *sld3*$^+$/*sld3*Δ*C* diploid strain, the *Spe*I-*Bam*HI fragment (encoding 65–600 amino acids and the *Nde*I site before the stop codon) of Sld3 was inserted into pBS-*sld3*-kan-DW to make pBS-*sld3*Δ*C*-kan-DW, and the *Spe*I-*Kpn*I fragment was used for transformation of a diploid strain TNF1879. The *Spe*I-*Nde*I fragment encoding 65–600 amino acids of Sld3 excised from pBS-*sld3*Δ*C*-kan-DW and the *Nde*I-*Bam*HI fragment encoding 1–648 amino acids of Cut5 were inserted in place of the *Spe*I-*Bam*HI site pBS-*sld3–9A-ura4*$^+$ to make pBS-*sld3*Δ*C-cut5-ura4*$^+$. The pBS-*sld3-cut5*Δ*N-ura4*$^+$ was made by similar replacement with the *Xho*I-*Nde*I fragment encoding 616–699 amino acids of Sld3 and the *Nde*I-*Bam*HI fragment encoding 191–648 amino acids of Cut5. To generate MF63 and MF48, the *Spe*I-*Kpn*I fragment of pBS-*sld3*Δ*C-cut5-ura4*$^+$ and *Xho*I-*Kpn*I fragment of pBS-*sld3-cut5*Δ*N-ura4*$^+$ were used to transform HM83, and the endogenous *cut5*$^+$ was replaced by the *kanMX6* gene.

MF70 carrying *leu1*$^+$::*Pnmt81-drc1*$^+$ was constructed by crossing HM19 with ENY165, and the endogenous *drc1*$^+$ was replaced by the *hphMX6* gene. For construction of the integration plasmid, the *Pst*I-*Hin*dIII fragment carrying the 297th amino acid through the downstream region of *drc1*$^+$ and a *Hin*dIII-*Xho*I fragment containing a downstream region of *drc1*$^+$ were PCR amplified using primer sets P11 and P12, and P13 and P14, respectively, and cloned into

Strain	Genotype	Source
MF3	*h⁻ sld3::sld3-4A-kanMX6*	This study
MF7	*h⁻ sld3::sld3-9A-kanMX6*	This study
MF9	*h⁻ sld3::sld3⁺-kanMX6*	This study
MF10	*h⁺ sld3::sld3-5A-kanMX6*	This study
MF11	*h⁻ sld3::sld3-5A-kanMX6*	This study
MF20	*h⁻ sld3::sld3-9A-kanMX6 leu1–32*	This study
MF23	*h⁺ sld3::sld3-5D-ura4⁺ ura4-D18*	This study
MF26	*h⁺ sld3::sld3-N4A-ura4⁺ ura4-D18*	This study
MF27	*h⁻ sld3::sld3⁺-kanMX6 cdc25–22*	This study
MF29	*h⁻ sld3::sld3-5A-kanMX6 cdc25–22*	This study
MF31	*h⁺ sld3::sld3-5A-ura4⁺ ura4-D18*	This study
MF38	*h⁻ sld3::sld3-9A-5flag-ura4⁺ cdc25-22 cut5::cut5-13myc-kanMX6*	This study
MF48	*h⁺ sld3::sld3⁺-cut5ΔN-ura4⁺ cut5::kanMX6*	This study
MF51	*h⁺/h⁻ sld3::sld3ΔC-kanMX6/sld3⁺ ade6-M210/ade6-M216*	This study
MF57	*h⁻ sld3::sld3-9A-5flag-ura4⁺ cdc10-129*	This study
MF62	*h⁺ sld3::sld3ΔC-cut5-ura4⁺ cut5::kanMX6*	This study
MF63	*h⁻ sld3::sld3ΔC-cut5-ura4⁺ cut5::kanMX6*	This study
MF64	*h⁻ sld3::sld3⁺-kanMX6 ade6Δ-D ura4-D18 leu1-32 ChL[ubcp4::LEU2::chk1 spcc1322.09::ura4⁺ ade6⁺]*	This study
MF65	*h⁻ sld3::sld3–5A-kanMX6 ade6Δ-D ura4-D18 leu1-32 ChL[ubcp4::LEU2::chk1 spcc1322.09::ura4⁺ ade6⁺]*	This study
MF66	*h⁻ sld3::sld3-9A-kanMX6 ade6Δ-D ura4-D18 leu1-32 ChL[ubcp4::LEU2::chk1 spcc1322.09::ura4⁺ ade6⁺]*	This study
MF70	*h⁻ drc1::drc1-ura4⁺ leu1⁺:Pnmt81-drc1-2HA6His*	This study
MF74	*h⁻ drc1::hphMX6 leu1⁺:Pnmt81-drc1-2HA6His sld3::sld3-5flag cut5::cut5-13myc-kanMX6 cdc25-22*	This study
MF76	*h⁻ drc1::hphMX6 leu1⁺:Pnmt81-drc1-2HA6His ura4-D18 cdc45::flag-cdc45 cdc25-22*	This study
MF92	*h⁻ drc1::drc1-T111A-ura4⁺ leu1⁺:Pnmt81-drc1-2HA6His cd45::flag-cdc45 cdc25-22*	This study
MF94	*h⁻ drc1::drc1-T111E-ura4⁺ leu1⁺:Pnmt81-drc1-2HA6His cdc45::flag-cdc45 cdc25-22*	This study
MF95	*h⁻ leu1⁺:Pnmt81-drc1-2HA6His sld3::sld3-5flag cut5::cut5-13myc-kanMX6 cdc25-22*	This study
MF96	*h⁻ drc1::drc1T111A-ura4⁺ leu1⁺:Pnmt81-drc1-2HA6 His sld3::sld3-5flag cut5::cut5-13myc-kanMX6 cdc25-22*	This study
MF99	*h⁻ drc1::drc1-T111A-ura4⁺ leu1⁺:Pnmt81-drc1-2HA6His*	This study
MF101	*h⁻ drc1::drc1-T111E-ura4⁺ leu1⁺:Pnmt81-drc1-2HA6His*	This study
MF112	*h⁻ sld3::sld3-4A636-kanMX6*	This study
MF113	*h⁻ sld3::sld3-4A650-kanMX6*	This study
MF114	*h⁻ sld3::sld3-4A673-kanMX6*	This study
MF115	*h⁻ sld3::sld3-4A690-kanMX6*	This study
HM2298	*h⁻ sld3::sld3-5flag cdc25-22 cut5::cut5-13myc-kanMX6*	Lab stock
HM19	*h⁻ 972*	Lab stock
HM20	*h⁺ 975*	Lab stock
HM83	*h⁺ ura4-D18*	Lab stock
HM3732	*h⁻ leu1-32*	Lab stock

[a]Drexel University College of Medicine, Philadelphia, PA.

TABLE 1: ***S. pombe*** **strains used in this study.**

(Continues)

Strain	Genotype	Source
HM513	*h⁺ sld3-10 leu1-32*	Lab stock
HM860	*h⁺ hsk1-89 leu1-32*	Lab stock
HM2080	*h⁻ psf3-1 leu1-32*	Lab stock
RY139	*h⁺ sld3::sld3-5flag cdc10-129*	Lab stock
TNF1610	*h⁻ ade6Δ-D ura4-D18 leu1-32*	Lab stock
	ChL[ubcp4::LEU2::chk1 spcc1322.09::ura4⁺ ade6⁺]	
TNF1879	*h⁺/h⁻ ade6-M210/ade6-M216*	Lab stock
ENY165	*h⁺ drc1::kan leu1⁺:Pnmt81-drc1-2HA6His ura4-D18 his7-366 ade6-M210 or ade6-M216*	Eishi Noguchi[a]

TABLE 1: *S. pombe* strains used in this study. (Continued)

*Pst*I-*Xho*I sites of pBS to make pBS-*drc1*DW. The *ura4⁺* gene was inserted at the *Hin*dIII site, resulting in pBS-*drc1*DW-*ura4⁺*. A 1.57-kb fragment containing the entire *drc1⁺* was PCR amplified using primers P15 and P16 and cloned into the *Xba*I site of pBluescript II KS+ to form pBS-*drc1-Xba*. The *Xba*I-*Pst*I fragment encoding the 1–297 amino acids of Drc1 was excised from pBS-*drc1-Xba* and inserted into the *Xba*I-*Pst*I sites of pBS-*drc1*DW-*ura4⁺* to generate pBS-*drc1-ura4⁺*. A *drc1* fragment carrying the *T111A* substitution was PCR amplified using primers P17 and P18, and then the products and P20 were used as primers for the second PCR reaction. The *Sal*I-*Pst*I fragment excised from the second PCR product was inserted in place of the corresponding fragment of pBS-*drc1-ura4⁺* to form pBS-*drc1-T111A-ura4⁺*. The pBS-*drc1-T111E-ura4⁺* was similarly constructed using primer sets P17 with P19 for the first PCR

No.	Name	5′-Sequence-3′	Source
P1	sld3 DW F	AAAGAATTCAAGCTTCTTTCTCAGCTCGTGTAG	This study
P2	sld3 DW2 R	AAAGGTACCGCAGTATCATTATTTCAT	This study
P3	*Bgl*IIx-*Sma*I-x*Pst*I 1	GATCCGAAAACCCGGGTGCA	This study
P4	*Bgl*IIx-*Sma*I-x*Pst*I 2	CCCGGGTTTTCG	This study
P5	SL3-F	GGGGTACCATATGAATAACGACCATGCTTC	lab stock
P6	sld3 Bm-698A R	AAAGGATCCTCAAGGAGCGGCTGATTT	This study
P7	sld3 140A R	ATTGAATTCTGTGAAGTTCCTTTTTTAACAAACTAGGTGCCATTAAAGAG	This study
P8	sld3 201A R	TTTGGATCCCACGTGAACAGCTAGGAGCATAATCTT	This study
P9	sld3 267A-Bm F	AAAGGATCCACGTGACGTTAAATCTTTGTTGGACCATATTTACAATTCCTACTTT-TATCAACTATTGATGACCAAAGCACC	This study
P10	sld3 499A R	TAGAGGCCTCCGAATGAGGAGCAGAAG	This study
P11	drc1DW1 F	ACTGCTAGCAAAGATTCG	This study
P12	drc1DW1 R	AAAAAGCTTCCAGGTTTTATTGAATGC	This study
P13	drc1DW2 F	AAAAAGCTTAAATAGATTTTGTGGGTTTTTGAG	This study
P14	drc1DW2 R	AAACTCGAGCAAAACGTTCCAGTCTTAG	This study
P15	drc1 up F2	GCTCTAGACGTATGCGTAAACATTCAGC	This study
P16	drc1 dw R2	GCTCTAGAGGATACCACAAACTCATGATG	This study
P17	drc1 up F	AAATTGGGTCCAGGCAGTGC	This study
P18	drc1 T111A R	CTCGACGTGACAACTGTGGAGCAGGACC	This study
P19	drc1 T111E R	CTCGACGTGACAACTGTGGTTCAGGACC	This study
P20	drc1R	AAAGGATCCTTAGCTTCTGTGACGCCG	This study
P21	drc1mu F	GGGTCCAGGCAGTGCATT	This study
P22	drc1dw950 R	TACCACTGAGCTACAAGAGC	This study
P23	sld3 mu12 F	GTCTTTGAAGGTGATAGC	This study
P24	sld3-T690S698A-NdBm R	AAAGGATCCTCACATATGAGGAGCGGCTGATTTTTTTTTAACAGGTGCTGTAGG-GACACA	This study
P25	sld3-S698A-NdBm R	AAAGGATCCTCACATATGAGGAGCGGCTGATTTTTTTTTA	This study

TABLE 2: Primers used in this study.

reaction. The *Xba*I-*Xho*I fragment was used for transformation of MF76. The *ura4*$^+$ hygromycin-sensitive transformants were selected and examined for correct integration at the *drc1*$^+$ locus using primers P21 and P22.

Yeast two- and three-hybrid assays

The BD Matchmaker GAL4 Two-Hybrid System 3 (Clontech Laboratories, Mountain View, CA) was used for yeast two-hybrid analysis. Derivatives of pGADT7, a Gal4-DNA-binding-domain (DB) vector, and pGBKT7, an activation-domain (AD) vector, were constructed as follows. The *Nde*I-*Bam*HI fragment encoding full-length Sld3 was inserted into pGBKT7 and pGADT7 to make pGBKT7-Sld3 and pGADT7-Sld3, respectively. To construct pGBKT7-Sld3-9A, the *Spe*I-*Bam*HI fragment encoding 65–699 of pBS-*sld3-9A*-kan-DW was inserted in place of the *Spe*I-*Bam*HI fragment of pGBKT7-Sld3. The *Nde*I-*Bam*HI fragments encoding 1–600, 118–699, 201–699, 480–699, and 601–699 amino acids and the *Nde*I-*Bgl*II fragment encoding 1–480 of Sld3 were PCR amplified and cloned into pGBKT7. The *Nde*I-*Bam*HI fragments encoding Mcm2, Mcm3, Mcm4, Mcm6, Mcm7, Psf1, Psf2, Psf3, Sld5, Drc1, Mcm10, Cdc45, and Cut5, respectively, were cloned into pGADT7. The *Nde*I-*Bam*HI fragment encoding Mcm5 was cloned into pGBKT7. To construct pGADT7-Cut5-N, pGADT7-BRCT-N, and pGADT7-Cut5-C, the *Nde*I-*Bam*HI fragments encoding 1–300, 1–190, and 300–648 amino acids of Cut5 were PCR amplified and cloned into pGADT7, respectively. To identify the region of Mcm2 interacting with Sld3, the *Nde*I-*Bam*HI fragments encoding 1–204, 1–280, and 200–830 amino acids of Mcm2 were cloned into pGADT7. The *Nde*I-*Bam*HI fragment encoding Drc1 with or without an amino acid substitution for T111 was cloned into pGBKT7. A pair of pGBKT7 and pGADT7 derivatives was introduced into *S. cerevisiae* AH109 (*MATa, trp1-901, leu2-3, 112, ura3-52, his3-200, gal4Δ, gal80Δ, LYS2::GAL1UAS-GAL1TATA-HIS3, GAL2UAS-GAL2TATA-ADE2, URA3::MEL1UAS-MEL1TATA-lacZ, MEL1*) cells. Trp$^+$ Leu$^+$ transformants harboring both plasmids were selected on synthetic glucose medium (SD) lacking tryptophan and leucine (SD-WL). The interaction was analyzed by growth on low-stringent media lacking histidine (SD-WLH) or high-stringent media lacking histidine and adenine (SD-WLHA) at 30°C for 3–4 d. Probably because higher expression level from *ADE2* reporter gene is required for the growth on the media lacking adenine than that from *HIS3* reporter, the growth on SD-WLHA indicates a strong interaction that induces transcription from both reporter genes. When indicated, 2 mM 3-aminotriazole was added to SD-WLH (SD-WLH+3AT).

For three-hybrid assays, a pBridge (Clontech) vector was used instead of pGBKT7. To construct pBridge derivatives, the *Sma*I-*Bam*HI fragment encoding Sld3 or Sld3-9A was cloned into the first cloning site to generate a Gal4-DB fusion protein, and the *Nde*I-*Bam*HI fragment encoding Drc1, Drc1-T111A, Drc1-T111E, Cut5, or a partial fragment of Cut5 was inserted into the *Nde*I-*Bgl*II sites for expression of the third protein.

Cell cycle synchronization

To obtain synchronous cell populations released from G1 phase, *sld3*$^+$ and *sld3-9A* derivatives carrying the temperature-sensitive *cdc10-129* mutation in the E2F transcription factor were arrested at 36°C for 3.5 h and released at 20°C, which is the restrictive temperature for *sld3-9A*. To synchronize the cell cycle from M phase, *psf3-1* and *cdc2-33* derivatives carrying the cold-sensitive *nda3-KM311* mutation in β-tubulin (Hiraoka *et al.*, 1984) were incubated at 20°C for 4 h and released at 36°C. For synchronization from the G2/M boundary, *cdc25-22* and *cdc25-22 sld3-9A* cells were incubated at 36°C for 3 h and released at 20°C. Derivatives of *cdc25-22* carrying *drc1*$^+$ *Pnmt81-drc1*$^+$ and *drc1-T111A Pnmt81-drc1*$^+$ grown at 25°C were cultured for 5 h in the presence of thiamine (1 μg/ml) to repress the *nmt1* promoter and then synchronized from the G2/M boundary.

Trichloroacetic acid extraction of proteins and immunoblotting

S. pombe haploid cells (1×10^8 cells) were washed with 0.3 ml of cold 10% trichloroacetic acid (TCA), suspended in 0.15 ml of 10% TCA, and disrupted with glass beads using Micro Smash (Tomy Seiko, Tokyo, Japan) four times for 40 s each. The cell extracts were collected by centrifugation at 3000 rpm for 1 min, and then glass beads were washed with 0.25 ml of 5% TCA. The collected supernatant (0.4 ml) was kept on ice for 30 min, and then precipitates were collected by centrifugation at 5000 rpm for 10 min at 4°C. Proteins were eluted in 0.1 ml of elution buffer (4% SDS, 0.5 M Tris-HCl [pH 8.0]) at room temperature for 20 min and added to 0.1 ml of 2× SDS buffer (120 mM Tris-HCl [pH 6.8], 4% SDS, 20% glycerol, 10% β-mercaptoethanol), separated by SDS–PAGE, and transferred onto polyvinylidene difluoride membranes (Immobilon; Millipore, Billerica, MA). The membranes were incubated for 30 min at room temperature in Blocking One (Nacalai Tesque, Kyoto, Japan) and reacted with mouse anti–FLAG M2 (1:4000; Sigma-Aldrich, St. Louis, MO) and mouse anti–α-tubulin antibodies (Woods *et al.*, 1989) (1:2000) in TBST (10 mM Tris-HCl [pH 8.0], 150 mM NaCl, 0.05% Tween 20) containing 5% Blocking One overnight at 4°C, followed by reaction with Horseradish peroxidase–conjugated anti–mouse immunoglobulin G antibody (1:10,000; Jackson ImmunoResearch Laboratories, West Grove, PA). Signals were visualized with the West Pico and Femto Chemiluminescent Substrate (Pierce, Thermo Fisher Scientific, Rockford, IL).

Phosphatase treatment of TCA-extracted protein

For immunoprecipitation of the TCA-extracted Sld3-FLAG or FLAG-Drc1, 40-μl eluates were diluted in 960 μl of IP buffer (0.16% SDS, 20 mM Tris-HCl [pH 8.0], 2 mM EDTA, 150 mM NaCl, 0.1% Triton X-100) and incubated with 5 μl of anti–FLAG M2 antibody-conjugated agarose beads (Sigma-Aldrich) at 4°C for 2 h. The beads were washed three times with IP buffer lacking SDS and once with phosphatase buffer (50 mM Tris-Cl [pH 8.0], 100 mM NaCl, 0.1 mM EGTA, 2 mM dithiothreitol, 2 mM $MnCl_2$, 1% Triton X-100) and incubated with or without 200 U of λ protein phosphatase (New England BioLabs, Ipswich, MA) at 30°C for 30 min. Proteins were eluted with 50 μl of 1× SDS buffer at 95°C for 2 min, separated by SDS–PAGE, and analyzed by Western blotting with mouse anti–FLAG M2.

Preparation of proteins for mass spectrometry analysis

HM3732 harboring pREP81-*flag-drc1* or pREP81-*sld3-flag* was grown to 1×10^7 cells/ml. The 1×10^9 cells were TCA extracted, and the TCA precipitates were eluted with 1 ml of elution buffer. FLAG-Drc1 or Sld3-FLAG was immunoprecipitated from the eluates using 10 μl of anti–FLAG M2 agarose beads as described earlier, and then the beads were washed six times with IP buffer lacking SDS. Purified proteins were eluted with 20 μl of 2× SDS buffer, separated by SDS–PAGE, and visualized by Coomassie Brilliant Blue staining. The bands corresponding to FLAG-Drc1 or Sld3-fLAG were excised, in-gel digested with trypsin, and analyzed by mass spectrometry.

Mass spectrometry and data analysis

Liquid chromatography/tandem mass spectrometry (MS/MS) analysis was performed as described (Nozawa *et al.*, 2010). The raw data

files were analyzed using Mascot (Matrix Science, Boston, MA), and phosphorylated peptides were validated manually.

Chromatin immunoprecipitation

Fission yeast cells (2×10^8) were fixed in 1% formaldehyde for 15 min at room temperature and then in 125 mM glycine for 5 min. After being washed twice with cold water and once with 1× phosphate-buffered saline, the cells were suspended in 0.4 ml of lysis buffer (50 mM Tris-HCl [pH 8.0], 280 mM NaCl, 1 mM EDTA, 1% Triton X-100, 0.1% sodium deoxycholate, 1 mM phenylmethylsulfonyl fluoride, and proteinase inhibitor cocktail [Sigma-Aldrich]). The cells were disrupted with glass beads using Micro Smash, and the extracts were sonicated three times for 10 s each (Sonifier; Branson, Danbury, CT). The supernatant obtained by centrifugation at 14,000 rpm for 20 min was used for immunoprecipitation with Dynal magnetic beads (Invitrogen, Carlsbad, CA) conjugated with rabbit anti-Mcm6 (1:400), mouse anti–FLAG M2 monoclonal (1:400; Sigma-Aldrich), and mouse anti–myc 9E11 Ab1 monoclonal (1:200; Lab Vision, Thermo Fisher Scientific, Fremont, CA) antibodies. DNA prepared from whole-cell extracts or immunoprecipitated fractions was analyzed by real-time PCR using SYBR green I in a 7300 real-time PCR System (Applied Biosystems, Foster City, CA). Two sets of primers were used to amplify a segment in the *ars2004* and adjacent nonorigin (non-ARS) regions on chromosome II.

The DNA sequences of these primers are as follows:

ars2004-66-F (5′-CGGATCCGTAATCCCAACAA-3′)
ars2004-66-R (5′-TTTGCTTACATTTTCGGGAACTTA-3′)
nonARS-70-F (5′-TACGCGACGAACCTTGCATAT-3′)
nonARS-70-R (5′-TTATCAGACCATGGAGCCCATT-3′)

Ch-L minichromosome assays

sld3-5A and *sld3-9A* mutations were introduced into the TNF1610 strain harboring a minichromosome Ch-L by transformation. Ch-L minichromosome assays were performed at 30°C as described previously (Nakamura *et al*., 2008). Because growth of *sld3-5A* and *sld-9A* derivatives was slightly slower than that of *sld3*$^+$, they were incubated for a day longer than the wild type on YE3S plates and 5-fluoroorotic acid plates containing adenine and leucine.

ACKNOWLEDGMENTS

We thank Hiroyuki Araki and Makoto Hayashi for critical reading of the manuscript and Eishi Noguchi for strains and plasmids. We thank Natsuko Shirai and Sachiko Shibata for technical assistance in mass spectrometry analysis. We are grateful to Shingo Azuma, Keiko Matsuda, Mitsuharu Takabayashi, and Tomonori Uchida for construction of strains and plasmids. This study was supported by a Grant-in-Aid from the Ministry of Education, Science, Technology, Sports, and Culture, Japan, to H.M.

REFERENCES

Balestrini A, Cosentino C, Errico A, Garner E, Costanzo V (2010). GEMC1 is a TopBP1-interacting protein required for chromosomal DNA replication. Nat Cell Biol 12, 484–491.

Bell SP, Dutta A (2002). DNA replication in eukaryotic cells. Annu Rev Biochem 71, 333–374.

Booher RN, Alfa CE, Hyams JS, Beach DH (1989). The fission yeast cdc2/cdc13/suc1 protein kinase: regulation of catalytic activity and nuclear localization. Cell 58, 485–497.

Bruck I, Kaplan D (2009). Dbf4-Cdc7 phosphorylation of Mcm2 is required for cell growth. J Biol Chem 284, 28823–28831.

Chowdhury A *et al*. (2010). The DNA unwinding element binding protein DUE-B interacts with Cdc45 in preinitiation complex formation. Mol Cell Biol 30, 1495–1507.

Diffley JF (2004). Regulation of early events in chromosome replication. Curr Biol 14, R778–R786.

Diffley JF, Cocker JH, Dowell SJ, Rowley A (1994). Two steps in the assembly of complexes at yeast replication origins in vivo. Cell 78, 303–316.

Du LL, Nakamura TM, Russell P (2006). Histone modification-dependent and -independent pathways for recruitment of checkpoint protein Crb2 to double-strand breaks. Genes Dev 20, 1583–1596.

Esashi F, Yanagida M (1999). Cdc2 phosphorylation of Crb2 is required for reestablishing cell cycle progression after the damage checkpoint. Mol Cell 4, 167–174.

Gambus A, Jones RC, Sanchez-Diaz A, Kanemaki M, van Deursen F, Edmondson RD, Labib K (2006). GINS maintains association of Cdc45 with MCM in replisome progression complexes at eukaryotic DNA replication forks. Nat Cell Biol 8, 358–366.

Garcia V, Furuya K, Carr AM (2005). Identification and functional analysis of TopBP1 and its homologs. DNA Repair (Amst) 4, 1227–1239.

Glover JN, Williams RS, Lee MS (2004). Interactions between BRCT repeats and phosphoproteins: tangled up in two. Trends Biochem Sci 29, 579–585.

Hashimoto Y, Takisawa H (2003). *Xenopus* Cut5 is essential for a CDK-dependent process in the initiation of DNA replication. EMBO J 22, 2526–2535.

Hiraoka Y, Toda T, Yanagida M (1984). The *NDA3* gene of fission yeast encodes β-tubulin: a cold-sensitive *nda3* mutation reversibly blocks spindle formation and chromosome movement in mitosis. Cell 39, 349–358.

Kamimura Y, Tak YS, Sugino A, Araki H (2001). Sld3, which interacts with Cdc45 (Sld4), functions for chromosomal DNA replication in *Saccharomyces cerevisiae*. EMBO J 20, 2097–2107.

Kanemaki M, Labib K (2006). Distinct roles for Sld3 and GINS during establishment and progression of eukaryotic DNA replication forks. EMBO J 25, 1753–1763.

Kubota Y, Takase Y, Komori Y, Hashimoto Y, Arata T, Kamimura Y, Araki H, Takisawa H (2003). A novel ring-like complex of *Xenopus* proteins essential for the initiation of DNA replication. Genes Dev 17, 1141–1152.

Kumagai A, Shevchenko A, Dunphy WG (2010). Treslin collaborates with TopBP1 in triggering the initiation of DNA replication. Cell 140, 349–359.

Lopez-Mosqueda J, Maas NL, Jonsson ZO, Defazio-Eli LG, Wohlschlegel J, Toczyski DP (2010). Damage-induced phosphorylation of Sld3 is important to block late origin firing. Nature 467, 479–483.

Machida YJ, Hamlin JL, Dutta A (2005). Right place, right time, and only once: replication initiation in metazoans. Cell 123, 13–24.

Masumoto H, Muramatsu S, Kamimura Y, Araki H (2002). S-Cdk-dependent phosphorylation of Sld2 essential for chromosomal DNA replication in budding yeast. Nature 415, 651–655.

Masumoto H, Sugino A, Araki H (2000). Dpb11 controls the association between DNA polymerases alpha and epsilon and the autonomously replicating sequence region of budding yeast. Mol Cell Biol 20, 2809–2817.

Matsuno K, Kumano M, Kubota Y, Hashimoto Y, Takisawa H (2006). The N-terminal noncatalytic region of *Xenopus* RecQ4 is required for chromatin binding of DNA polymerase alpha in the initiation of DNA replication. Mol Cell Biol 26, 4843–2852.

Moreno S, Klar A, Nurse P (1991). Molecular genetic analysis of fission yeast *Schizosaccharomyces pombe*. Methods Enzymol 194, 795–823.

Moyer SE, Lewis PW, Botchan MR (2006). Isolation of the Cdc45/Mcm2-7/GINS (CMG) complex, a candidate for the eukaryotic DNA replication fork helicase. Proc Natl Acad Sci USA 103, 10236–10241.

Muramatsu S, Hirai K, Tak YS, Kamimura Y, Araki H (2010). CDK-dependent complex formation between replication proteins Dpb11, Sld2, Polε, and GINS in budding yeast. Genes Dev 24, 602–612.

Nakajima R, Masukata H (2002). SpSld3 is required for loading and maintenance of SpCdc45 on chromatin in DNA replication in fission yeast. Mol Biol Cell 13, 1462–1472.

Nakamura K *et al*. (2008). Rad51 suppresses gross chromosomal rearrangement at centromere in *Schizosaccharomyces pombe*. EMBO J 27, 3036–3046.

Noguchi E, Shanahan P, Noguchi C, Russell P (2002). CDK phosphorylation of Drc1 regulates DNA replication in fission yeast. Curr Biol 12, 599–605.

Nozawa RS, Nagao K, Masuda HT, Iwasaki O, Hirota T, Nozaki N, Kimura H, Obuse C (2010). Human POGZ modulates dissociation of HP1alpha from mitotic chromosome arms through Aurora B activation. Nat Cell Biol 12, 719–727.

Pacek M, Tutter AV, Kubota Y, Takisawa H, Walter JC (2006). Localization of MCM2-7, Cdc45, and GINS to the site of DNA unwinding during eukaryotic DNA replication. Mol Cell 21, 581–587.

Patel PK, Kommajosyula N, Rosebrock A, Bensimon A, Leatherwood J, Bechhoefer J, Rhind N (2008). The Hsk1(Cdc7) replication kinase regulates origin efficiency. Mol Biol Cell 19, 5550–5558.

Remus D, Beuron F, Tolun G, Griffith JD, Morris EP, Diffley JF (2009). Concerted loading of Mcm2-7 double hexamers around DNA during DNA replication origin licensing. Cell 139, 719–730.

Saka Y, Esashi F, Matsusaka T, Mochida S, Yanagida M (1997). Damage and replication checkpoint control in fission yeast is ensured by interactions of Crb2, a protein with BRCT motif, with Cut5 and Chk1. Genes Dev 11, 3387–3400.

Saka Y, Fantes P, Sutani T, McInerny C, Creanor J, Yanagida M (1994). Fission yeast *cut5* links nuclear chromatin and M phase regulator in the replication checkpoint control. EMBO J 13, 5319–5329.

Sanchez-Pulido L, Diffley JF, Ponting CP (2010). Homology explains the functional similarities of Treslin/Ticrr and Sld3. Curr Biol 20, R509–510.

Sangrithi MN, Bernal JA, Madine M, Philpott A, Lee J, Dunphy WG, Venkitaraman AR (2005). Initiation of DNA replication requires the RECQL4 protein mutated in Rothmund–Thomson syndrome. Cell 121, 887–898.

Sansam CL, Cruz NM, Danielian PS, Amsterdam A, Lau ML, Hopkins N, Lees JA (2010). A vertebrate gene, ticrr, is an essential checkpoint and replication regulator. Genes Dev 24, 183–194.

Sheu YJ, Stillman B (2010). The Dbf4-Cdc7 kinase promotes S phase by alleviating an inhibitory activity in Mcm4. Nature 463, 113–117.

Tak YS, Tanaka Y, Endo S, Kamimura Y, Araki H (2006). A CDK-catalysed regulatory phosphorylation for formation of the DNA replication complex Sld2-Dpb11. EMBO J 25, 1987–1996.

Tanaka S, Umemori T, Hirai K, Muramatsu S, Kamimura Y, Araki H (2007). CDK-dependent phosphorylation of Sld2 and Sld3 initiates DNA replication in budding yeast. Nature 445, 328–332.

Woods A, Sherwin T, Sasse R, MacRae TH, Baines AJ, Gull K (1989). Definition of individual components within the cytoskeleton of *Trypanosoma brucei* by a library of monoclonal antibodies. J Cell Sci 93 (Pt 3), 491–500.

Yabuuchi H, Yamada Y, Uchida T, Sunathvanichkul T, Nakagawa T, Masukata H (2006). Ordered assembly of Sld3, GINS and Cdc45 is distinctly regulated by DDK and CDK for activation of replication origins. EMBO J 25, 4663–4674.

Yamada Y, Nakagawa T, Masukata H (2004). A novel intermediate in initiation complex assembly for fission yeast DNA replication. Mol Biol Cell 15, 3740–3750.

Zegerman P, Diffley JF (2007). Phosphorylation of Sld2 and Sld3 by cyclin-dependent kinases promotes DNA replication in budding yeast. Nature 445, 281–285.

Zegerman P, Diffley JF (2010). Checkpoint-dependent inhibition of DNA replication initiation by Sld3 and Dbf4 phosphorylation. Nature 467, 474–478.